



## RESEARCH LETTER

10.1002/2013GL058320

## Key Points:

- Strong semidiurnal and diurnal internal tide beams are observed in Kauai Channel
- Energy at  $M_2$  subharmonic ( $M_2/2$ ) is weak at all depths, including within  $M_2$  beam
- Bispectra can falsely indicate nonlinear interactions if diurnal tides are present

## Correspondence to:

Sherry H. Chou,  
schou@hawaii.edu

## Citation:

Chou, S. H., D. S. Luther, M. D. Guiles, G. S. Carter, and T. Decloedt (2014), An empirical investigation of nonlinear energy transfer from the  $M_2$  internal tide to diurnal wave motions in the Kauai Channel, Hawaii, *Geophys. Res. Lett.*, 41, doi:10.1002/2013GL058320.

Received 29 OCT 2013

Accepted 19 DEC 2013

Accepted article online 26 DEC 2013

## An empirical investigation of nonlinear energy transfer from the $M_2$ internal tide to diurnal wave motions in the Kauai Channel, Hawaii

Sherry H. Chou<sup>1</sup>, Douglas S. Luther<sup>1</sup>, Martin D. Guiles<sup>1</sup>, Glenn S. Carter<sup>1</sup>, and Thomas Decloedt<sup>1</sup>

<sup>1</sup>Department of Oceanography, School of Ocean and Earth Science and Technology, University of Hawaii at Manoa, Honolulu, Hawaii, USA

**Abstract** Current profiles are examined for evidence of nonlinear energy transfers from the  $M_2$  internal tide to diurnal waves. The 6 month records, unlike shorter records, produce well-resolved velocity and shear spectra that consistently exhibit maxima at the diurnal tides  $O_1$  and  $K_1$ , with a minimum at the intermediate  $M_2$  subharmonic,  $M_2/2$ . The ratio of velocity spectral energy at  $M_2/2$  and  $M_2$  is quantified, providing a needed modeling benchmark. Bispectra and bicoherences imply a negligible  $[-M_2/2, -M_2/2, -M_2]$  triad interaction, but possibly a significant interaction for the  $[-O_1, -K_1, -M_2]$  triad. Numerical simulations, however, indicate that  $O_1$  and  $K_1$  signals are from internal tides. Tests with synthetic data, linear tides plus random noise, reveal that bispectrum and bicoherence estimators can yield significant values, thus misleading results. Therefore, resolving the diurnal tides from  $M_2/2$  is essential to meaningfully assess nonlinear transfer of energy from  $M_2$  to diurnal waves.

### 1. Introduction

The flow of energy through the internal wave (IW) field has taken on renewed importance due to the evidence suggesting that IWs drive significant diapycnal mixing in the deep ocean, helping to maintain the abyssal density stratification against the influx of deep and bottom waters formed at high latitudes. The internal tides are considered to be among the most important IWs in this role. Tide models that assimilate satellite altimeter data indicate that up to 1 TW of barotropic tide power is dissipated in the deep ocean over rough topography [e.g., *Egbert and Ray*, 2000], possibly accounting for 50–100% of the power needed to maintain the abyssal stratification [e.g., *Munk and Wunsch*, 1998; *Decloedt and Luther*, 2010]. Some of the barotropic tide dissipation directly results in localized mixing, but most of it drives internal waves (internal tides) that propagate away. The principal locations and pathways (in physical and frequency-wave number spaces) of the subsequent internal tide dissipation are still unknown [e.g., *Garrett and Kunze*, 2007; *MacKinnon et al.*, 2013].

The internal tide energy cascade in wave number space can potentially span several orders of magnitude as energy is transferred from large-scale waves directly forced by the barotropic tides to smaller scale internal waves which are more easily dissipated [e.g., *Polzin*, 2004]. Nonlinear processes, of which the Parametric Subharmonic Instability (PSI) resonant triad wave-wave interaction is an example, have been conjectured to be the main mechanisms facilitating this energy cascade [e.g., *McComas and Bretherton*, 1977]. Numerical and observational studies have suggested that direct and rapid energy transfer from the large-scale  $M_2$  tide to small-scale oscillations at the  $M_2$  subharmonic ( $M_2/2$ , or  $M_1$ ) frequency can occur for a range of latitudes equatorward of  $\sim 29^\circ$  [e.g., *Hibiya and Nagasawa*, 2004; *Gerkema et al.*, 2006]. Specifically, studies around the Kauai Channel [e.g., *Carter and Gregg*, 2006; *Rainville and Pinkel*, 2006; *Sun and Pinkel*, 2013] and the Luzon Strait [e.g., *Xie et al.*, 2011; *Liao et al.*, 2012] have inferred from observations that PSI is an identifiable mechanism of nonlinear energy transfer, even at tropical latitudes ( $\sim 21^\circ$ N). The geographical extent of PSI acting on energetic internal tides is an important aspect of its relevance to diapycnal mixing in the global ocean.

Although there is substantial literature on the subject of PSI, numerical experiments have been highly idealized, and observational efforts usually have not explicitly distinguished nonlinearly produced  $M_1$  energy from diurnal tides, due to insufficient data lengths. The principal purpose of the present study is to quantify the energy at  $M_1$  relative to  $M_2$  internal tide energy, with a data set from the Hawaii Ocean Mixing Experiment (HOME) that is long enough to clearly resolve in frequency the energy in  $M_1$  horizontal currents as distinct from the principal diurnal  $O_1$  and  $K_1$  tidal currents.

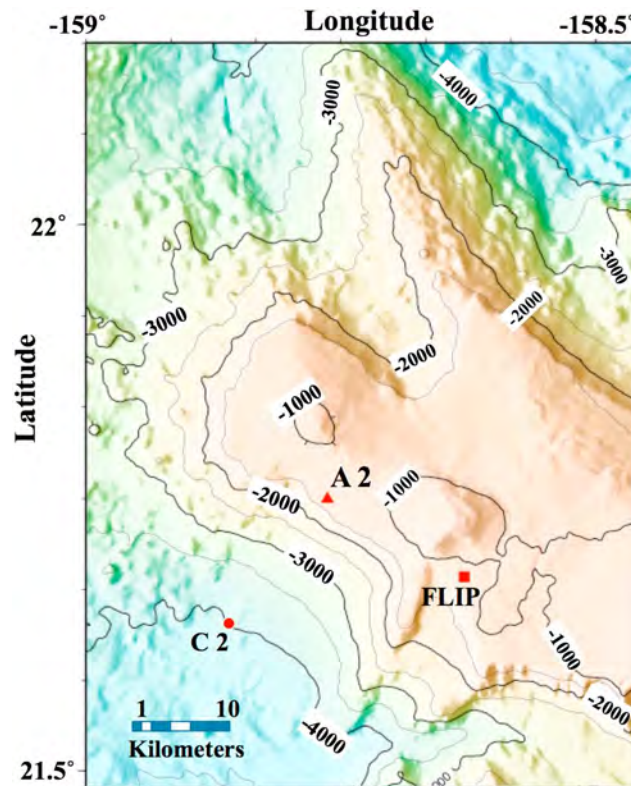


**Figure 1.** Location of the HOME A2 mooring (21.75°N, 158.75°W) is shown on a bathymetry map with contour lines every 500 m. Two other field locations, for the HOME C2 mooring [e.g., Carter *et al.*, 2008; Zilberman *et al.*, 2011] and the Floating Instrument Platform (FLIP) [e.g., Rainville and Pinkel, 2006; Sun and Pinkel, 2013], are also indicated.

A secondary purpose of this work is to provide a direct assessment of the occurrence of nonlinear interactions between  $M_2$  and diurnal waves in this unique HOME data set, using bispectral analysis. The HOME data have a vertical extent ( $\sim 1000$  m) that encompasses distinct, depth-limited beams of semidiurnal tide energy. Whether such vertically confined beams, with their higher vertical wave number content, result in more rapid transfers of energy from the principal tidal constituents to nonlinear harmonics than just low-vertical-mode constructs has not yet been determined observationally; in idealized numerical models [e.g., Gerkema *et al.*, 2006; Simmons, 2008], both yield resonant nonlinear interactions.

## 2. Observations and Methods

The data set used in this study comes from two RDI Long Ranger acoustic Doppler current profilers (ADCPs) deployed from 16 November 2002 to 11 June 2003 at 746 m and 1314 m on the HOME A2 mooring in the Kauai Channel (Figure 1), where the water depth was  $\sim 1333$  m. The data have been cleaned following Boyd *et al.* [2005] and Guiles [2009]. To facilitate examination of internal wave motions, barotropic tidal currents are subtracted from measurements at all depths using the most up to date Oregon State University tidal inversion software (OTIS) [Egbert and Erofeeva, 2002] Regional Tidal Solution (Hawaii, 2010) for the Kauai Channel.

To optimize the accuracy of the discrete Fourier transform (DFT) for the diurnal band, data lengths that result in the least misalignment of DFT harmonics with  $O_1$ ,  $M_1$ , and  $K_1$  are calculated numerically [Chou, 2013], before estimating power spectral density (PSD). The chosen data length is 163.5 days (2 December 2002 to 15 May 2003), and a tapered (10% cosine) window is applied to the truncated time series prior to calculating DFTs for auto-spectra. In order to increase statistical reliability, the PSD estimates are averaged in frequency space (three points) as well as depth (80 m). Additional degrees of freedom (DOF) from depth averaging are calculated by estimating vertical coherence lengths for the horizontal velocity ( $\sim 96$  m) and vertical shear ( $\sim 40$  m) fields [Chou, 2013].

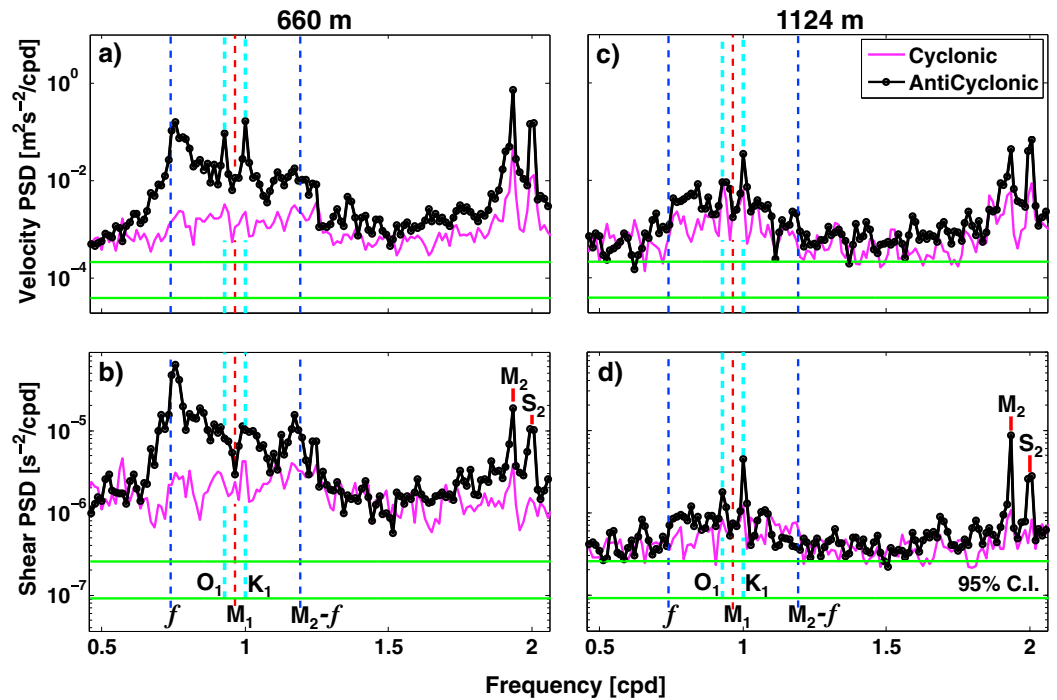


**Figure 2.** Rotary spectra of horizontal velocity and vertical shear at (a, b) 660 m and (c, d) 1124 m are shown with 95% confidence intervals (C.I.); every other plotted point is independent.

Many observational studies investigating nonlinear interactions between the  $M_2$  tide and  $M_1$  at tropical latitudes have utilized bispectral techniques in addition to auto-spectral analysis [e.g., Carter and Gregg, 2006; Liao et al., 2012]. Expectation values necessary for bispectral analysis [e.g., Elgar and Guza, 1988] are most often calculated through ensemble averaging in the time domain, and this has been done for short ( $\sim 10$  days) [Carter and Gregg, 2006] as well as long ( $> 8$  months) [Liao et al., 2012] data sets, at the cost of reduced frequency resolution. In order to maintain sufficient resolution to distinguish between  $M_1$  and diurnal tidal constituents  $O_1$  and  $K_1$ , expectation values for this study are calculated with only 1 time segment, using a two-dimensional ( $5 \times 5$ ) filter in frequency space and depth averaging over 80 m [Chou, 2013].

### 3. Results

#### 3.1. Spectral Energy of Velocity and Shear

The DFT of a 163.5 day time series yields transform harmonics separated by  $\sim 0.006$  cycles/day (cpd), permitting clear discrimination of  $O_1$  (0.930 cpd),  $M_1$  (0.966 cpd), and  $K_1$  (1.003 cpd) wave motions in frequency space (e.g., Figure 2). The velocity auto-spectra show distinct, significant peaks for the four main semidiurnal and diurnal tidal constituents, and a noticeable valley at the  $M_1$  frequency. Near-inertial waves, probably directly wind generated, are appropriately prominent (the local inertial frequency is indicated as  $f$ , as usual). Such waves, being highly intermittent in time, tend to have a broad frequency bandwidth, which extends well above the local  $f$  as the waves propagate south from their origins. This might account for much of the apparent “background” level of energy in the diurnal band. At 660 m on the HOME A2 mooring, the broad near-inertial peak of the 8 m vertical shear field (Figure 2b) has increased in prominence compared to the velocity spectrum (Figure 2a) since the shear spectrum is weighted toward larger vertical wave numbers, which tend to dominate the near-inertial waves. Depending on depth, the spectral peaks near  $M_2 - f$  are attributed to either vertical advection of near-inertial motions by the  $M_2$  internal tide or nonlinear wave-wave interactions between near-inertial waves and the  $M_2$  internal tide [Guiles, 2009].

Deeper in the water column, spectral energy is decreased overall (e.g., at 1124 m; Figures 2c and 2d), but peaks at the tidal frequencies are still clearly distinguishable in both velocity and shear spectra. Spectral levels

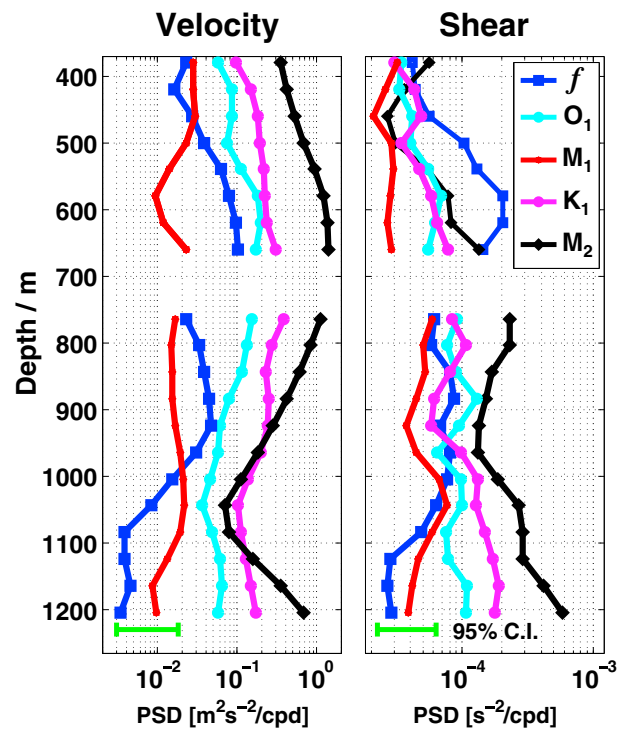


**Figure 3.** Velocity and shear power spectral densities (PSDs) are calculated as the mean of three adjacent discrete Fourier transform harmonics centered at the noted frequency and scaled by the buoyancy frequency  $N$  according to WKB theory [Leaman and Sanford, 1975]. Depth averaging is done with 50% overlapping windows spanning 80 m.

at  $M_1$  remain lower than at  $O_1$  and  $K_1$ . The shear spectrum is no longer dominated by inertial-frequency motions below 700 m (Figure 3), suggesting a lack of effective downward transport of small vertical scale near-inertial motions past the pycnocline. The velocity PSD profile in Figure 3 shows that  $M_2$  internal tide kinetic energy has a relative maximum near 700 m (due to an upward-propagating tide beam; e.g., Carter *et al.* [2008]), while in both velocity and shear, spectral energy at  $M_1$  is always lower than the energies at  $O_1$  and  $K_1$ . Within a 250 m depth range of strongest  $M_2$  tidal energy (550–800 m), the velocity PSD at  $M_1$  relative to  $M_2$  is approximately 0.013, with the 95% confidence interval (0.0063, 0.027) roughly a multiplicative factor of 2 around the estimate.

### 3.2. Bispectra and Bicoherence of Velocity

At 660 m, where the  $M_2$  internal tide is energetic and beam-like, elevated bispectral values (exceeding background levels by at least an order of magnitude) are found for potential resonant triads such as  $[-O_1, -K_1, -M_2]$  and  $[-K_1, -K_1, -K_2]$  (Figure 4a), where  $K_2$  is the lunisolar semidiurnal tidal constituent with twice the frequency of  $K_1$ , and negative frequencies denote anticyclonic rotation. In general, bispectra and bicoherence need to be considered together, with neither one sufficient by itself for indicating nonlinear interactions [e.g., Yao *et al.*, 1975; MacKinnon *et al.*, 2013]. A potential resonant triad may yield suggestive bispectral peaks without significant bicoherence (such as the  $[-K_1, -K_1, -K_2]$  triad), or significant bicoherence but negligible bispectral energy (such as the location of the maximum in Figure 4d, or the  $[+K_1, +O_1, +M_2]$  triad from Figure 3.11-3.12 of Chou [2013]). At this depth, only the frequency triplet  $[-O_1, -K_1, -M_2]$  has both elevated bispectral energy and bicoherence above the 90% significance level ( $\sim 0.76$ , calculated following Elgar and Guza [1988] with  $DOF \sim 8$ ).

Depth profiles of bispectral energy and bicoherence show that the frequency triplet  $[-O_1, -K_1, -M_2]$  consistently has both high bispectral and bicoherence values from 660 to 884 m (Figure 5). In contrast, the  $[-M_1, -M_1, -M_2]$  triad has bispectral values at least an order of magnitude less than those of  $[-O_1, -K_1, -M_2]$  throughout most of the water column, and its bicoherence values are generally below the 80% significance level ( $\sim 0.63$ ).

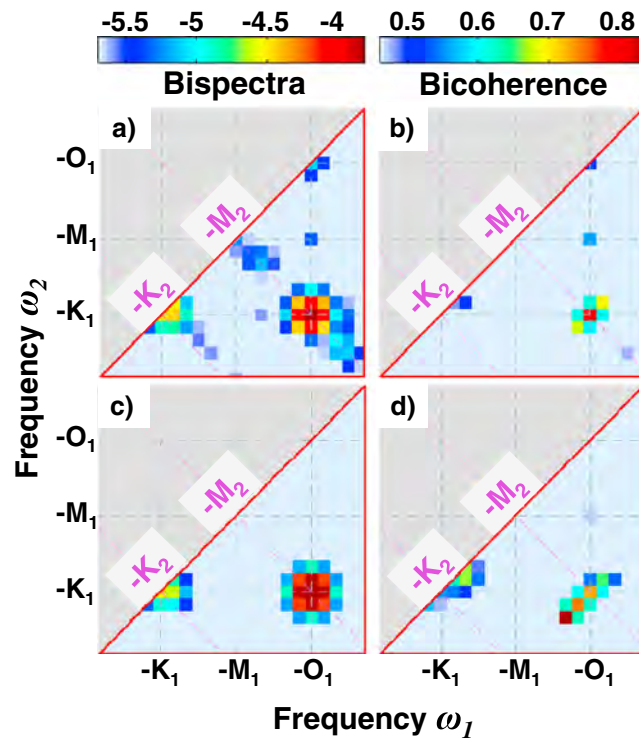


**Figure 4.** Bispectra (log scale) and bicoherence are calculated for complex velocity  $u + iv$  at 660 m on the (a, b) A2 mooring and (c, d) for synthetic data containing linear sinusoidal inputs at the eight major tidal frequencies (four diurnal and four semidiurnal). Horizontal and vertical axes correspond to the frequencies of the first and second waves of a triad ( $\omega_1, \omega_2$ ), respectively, and the diagonal axis corresponds to the sum frequency  $\omega_3 = \omega_1 + \omega_2$ . Relative tidal amplitudes and phases for the synthetic data are set according to the OTIS Regional Tidal Solution (Hawaii, 2010) at the A2 location, and white Gaussian noise is added at 10 decibels (signal-to-noise).

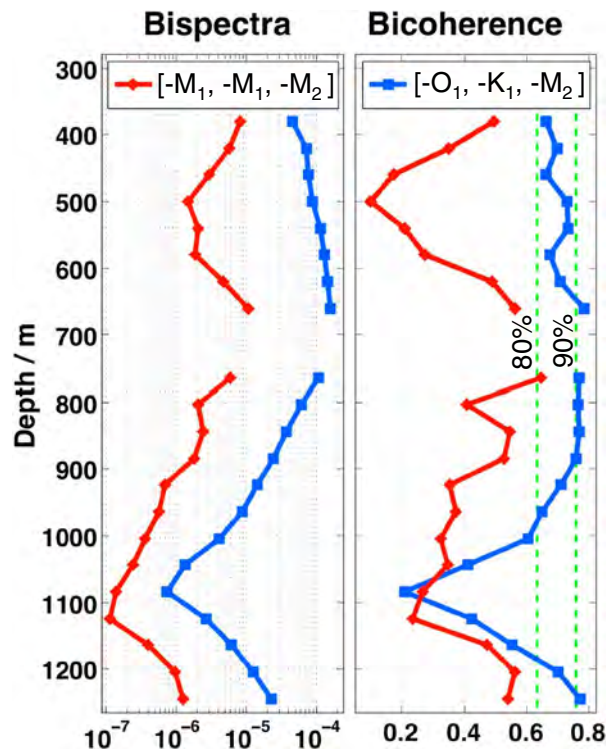


**Figure 5.** Bispectra and bicoherence of frequency triplets  $[-M_1, -M_1, -M_2]$  and  $[-O_1, -K_1, -M_2]$  are shown along with 80% and 90% significance levels (green dashed lines).

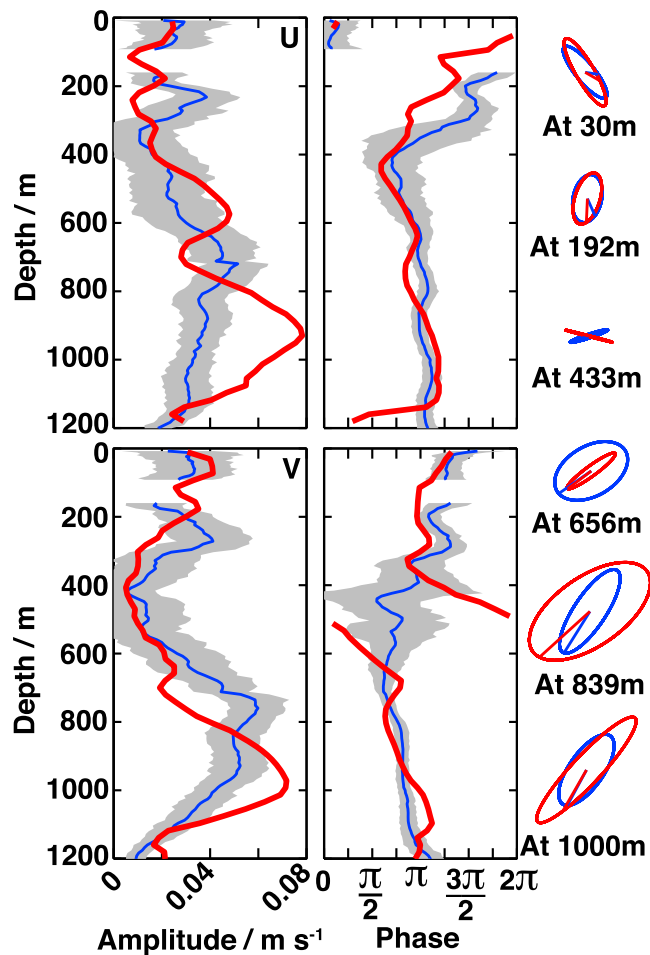


**Figure 6.** Harmonic fits of the  $K_1$  frequency are calculated using T\_TIDE [Pawlowicz et al., 2002] for 5 months of A2 mooring velocities (blue, with 95% C.I. in gray) and output from a 1 km resolution model (red). Results are consistent in both amplitude and phase, especially in the depth range where  $M_2$  tide is strongest (550–800 m).

#### 4. Discussion and Conclusions

Equatorward of the “critical latitude” where the inertial frequency equals  $M_1$ , there is no general consensus on the issue of which frequencies are preferred by resonant wave-wave triad interactions that transfer energy from a large-scale  $M_2$  internal tide (the primary wave) to lower frequency, small-scale secondary waves. In the case of PSI, analytical [e.g., Staquet and Sommeria, 2002] and numerical [e.g., Hazewinkel and Winters, 2011] studies suggest that the growth rate of secondary waves approaches a maximum as secondary wave frequencies approach equality. However, there are observational [e.g., Xie et al., 2011] and numerical [e.g., Nikurashin and Legg, 2011] studies that find  $M_2$ -forced secondary waves at frequencies  $f$  and  $M_2 - f$ , even at latitudes  $\sim 21^\circ$  (where  $\Delta\omega$ , the frequency separation between these two waves, is  $M_2 - 2f > 0.5$  cpd). Given that diurnal band spectral energy appears to be concentrated at  $O_1$  and  $K_1$  ( $\Delta\omega \sim 0.073$  cpd) for the A2 mooring data, we consider whether the bispectral and bicoherence evidence presented earlier supports a hypothesis of resonant nonlinear energy transfer from the  $M_2$  tide to internal wave motions at  $O_1$  and  $K_1$  (the  $M_2$  frequency equals the  $O_1$  plus  $K_1$  frequencies).

First, the magnitudes and vertical structures of observed diurnal currents are well predicted by an internal tide simulation model identical to that in Carter et al. [2008] except forced with only the  $K_1$  or  $O_1$  constituent. The similarity between  $K_1$  (and  $O_1$ , not shown) harmonic fits from the model and from A2 observations suggests that local generation of an internal tide is a sufficient explanation for the observed diurnal currents (Figure 6). Second, the maxima in the diurnal-band velocity PSD do not coincide with the semidiurnal maxima (Figure 7). Because both diurnal and semidiurnal internal tides emanate from the edges of the Kauai Channel Ridge crest, and the group velocity is more nearly horizontal at the lower frequency, the diurnal-band maxima

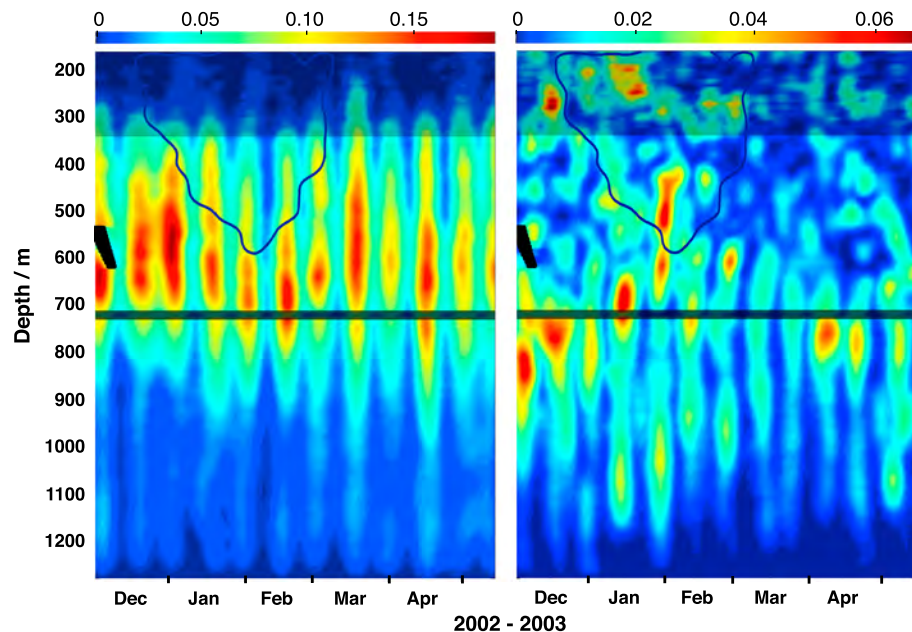


**Figure 7.** Semidiurnal-band (1.88–2.06 cpd, left panel) and diurnal-band (0.96–1.11 cpd, right panel) PSDs [ $\text{m}^2\text{s}^{-2}/\text{cpd}$ ] of A2 mooring velocities are calculated daily with a window of effective half width  $\sim 4.2$  days following *Guiles* [2009]. Locations of poor ADCP data quality are shaded. Strong background flow is marked by the thin blue contours, within which the 15 day-averaged meridional velocity exceeds 5 cm/s in amplitude.

tend to be deeper than the semidiurnal, though there are exceptions. As a whole, these observations suggest that sustained nonlinear interactions between the diurnal and semidiurnal bands at this location are unlikely.

The bispectral analyses presented earlier (Figures 4a and 4b) showed that the  $[-O_1, -K_1, -M_2]$  triad has both elevated bispectral energy and significant bicoherence throughout a depth range  $> 200$  m where the  $M_2$  tide is energetic and beam-like, evidence that has been interpreted as indicating nonlinear energy transfer in recent studies of PSI [e.g., *Xie et al.*, 2011; *Liao et al.*, 2012]. However, an experiment using the same bispectral techniques applied to a synthetic data set containing only deterministic tidal inputs and white Gaussian noise also resulted in elevated bispectral values and high bicoherence for the  $[-O_1, -K_1, -M_2]$  triad (Figures 4c and 4d), showing that these results do not always carry physical meaning [*Yao*, 1974]. A basic assumption of bispectral analysis is that the processes under study are stochastic and stationary, and it is unclear how the results should be interpreted for nearly deterministic signals such as internal tides. Tests of the bispectral technique can be performed with synthetic data for a given location (e.g., Figures 4c and 4d), or by using actual observations (a composite data set from different locations, for example) that do not have any real nonlinear interaction between semidiurnal and diurnal waves.

Although some observational studies attribute energy in the entire diurnal band to nonlinear transfers of energy from the  $M_2$  tide to waves of approximately  $M_1$  frequency, the analysis presented here strongly suggests that resolution of the diurnal internal tides from  $M_1$  is essential before attempting to assess nonlinear transfer of energy from  $M_2$  to diurnal waves. Within a 250 m depth range of strongest  $M_2$  tidal energy, the velocity PSD at  $M_1$  is approximately  $10^{-2}$  of the velocity PSD at  $M_2$ . This quantification of spectral energy at  $M_1$  provides a benchmark for comparison with numerical simulations of nonlinear energy transfers from the  $M_2$  internal tide to subharmonic waves [e.g., *Gerkema et al.*, 2006; *Simmons*, 2008]. If PSI or other nonlinear mechanisms are active in transferring energy at the A2 mooring from the semidiurnal internal tides to the diurnal band, they are so weak as to be of little consequence in either velocity or shear. The role of PSI and other nonlinear energy transfers in shaping the ocean's internal wave spectrum remains to be adequately quantified. Progress will require more realistic numerical simulations and comparable observations of adequate duration and spatial coverage.

## References

- Boyd, T. J., M. D. Levine, S. R. Gard, and W. Waldorf (2005), Mooring observations from the Hawaiian Ridge, *Rep. 197*, College of Oceanic and Atmospheric Sciences, Oregon State Univ., Corvallis, Ore.
- Carter, G. S., and M. C. Gregg (2006), Persistent near-diurnal internal waves observed above a site of  $M_2$  barotropic-to-baroclinic conversion, *J. Phys. Oceanogr.*, *36*, 11,036–11,052.

## Acknowledgments

We thank Captains Dan Arnsdorf and Tom Desjardins of R/V *Wecoma* and R/V *Revelle*, respectively, and their outstanding crews, as well as the many OSU and UH techs and students who assisted with the deployments and recoveries of the HOME moorings and with data processing. High-quality density profiles for Station Kaena were obtained from the Hawaii Ocean Time-series program, funded by the National Science Foundation (NSF). The HOME mooring program at UH was supported by NSF Grant OCE9819533, and the modeling work presented in this paper was supported by NSF Grant OCE0425347. We would also like to thank Mark Merrifield, Janet Becker, Eric Firing, and two anonymous reviewers for their helpful comments and suggestions. This work is dedicated to the memories of Murray Levine and Tim Boyd, who contributed greatly to the success of the HOME mooring deployments and interpretations, and with whom it was a distinct pleasure to work.

The Editor thanks two anonymous reviewers for assistance in evaluating this manuscript.

- Carter, G. S., M. A. Merrifield, J. M. Becker, K. Katsumata, M. C. Gregg, D. S. Luther, M. D. Levine, T. J. Boyd, and Y. L. Firing (2008), Energetics of M2 barotropic-to-baroclinic tidal conversion at the Hawaiian Islands, *J. Phys. Oceanogr.*, *38*, 2205–2223.
- Chou, S. (2013), An Empirical Investigation of Energy Transfer from the M2 tide to M2 Subharmonic Wave Motions in the Kauai Channel, M.S. thesis, Department of Oceanography, Univ. of Hawaii at Manoa, Honolulu, Hawaii.
- Decloedt, T., and D. S. Luther (2010), On a Simple Empirical Parameterization of Topography-Catalyzed Diapycnal Mixing in the Abyssal Ocean, *J. Phys. Oceanogr.*, *40*, 487–508.
- Egbert, G. D., and R. D. Ray (2000), Significant dissipation of tidal energy in the deep ocean inferred from satellite altimeter data, *Nature*, *405*, 775–778.
- Egbert, G. D., and S. Y. Erofeeva (2002), Efficient Inverse modeling of Barotropic Ocean Tides, *J. Atmos. Oceanic Technol.*, *19*, 183–204.
- Elgar, S., and R. T. Guza (1988), Statistics of Bicoherence, *IEEE Trans. Acoust. Speech Signal Process.*, *36*, 1668–1668.
- Garrett, C., and E. Kunze (2007), Internal Tide Generation in the Deep Ocean, *Annu. Rev. Fluid Mech.*, *39*, 57–87.
- Gerkema, T., C. Staquet, and P. Bouruet-Aubertot (2006), Decay of semi-diurnal internal-tide beams due to subharmonic resonance, *Geophys. Res. Lett.*, *33*, L08604, doi:10.1029/2005GL025105.
- Guiles, M. (2009), Energy Redistribution through Tidal and Inertial Wave Interaction, PhD dissertation, Department of Oceanography, Univ. of Hawaii at Manoa, Honolulu, Hawaii.
- Hazewinkel, J., and K. B. Winters (2011), PSI of the internal tide on a beta-plane: Flux divergence and near-inertial wave propagation, *J. Phys. Oceanogr.*, *41*, 1673–1682.
- Hibiya, T., and M. Nagasawa (2004), Latitudinal dependence of diapycnal diffusivity in the thermocline estimated using a finescale parameterization, *Geophys. Res. Lett.*, *31*, L01301, doi:10.1029/2003GL017998.
- Leaman, K., and T. B. Sanford (1975), Vertical energy propagation of inertial waves: A vector spectral analysis of velocity profiles, *J. Geophys. Res.*, *80*, 1975–1978.
- Liao, G., Y. Yuan, C. Yang, H. Chen, H. Wang, and W. Huang (2012), Current Observations of Internal Tides and Parametric Subharmonic Instability in Luzon Strait, *Atmos. Ocean*, *50*, 59–76.
- MacKinnon, J. A., M. H. Alford, O. Sun, R. Pinkel, Z. Zhao, and J. Klymak (2013), Parametric Subharmonic Instability of the Internal Tide at 29°N, *J. Phys. Oceanogr.*, *43*, 17–28.
- McComas, C. H., and F. P. Bretherton (1977), Resonant Interaction of Oceanic Internal Waves, *J. Geophys. Res.*, *82*, 1397–1412.
- Munk, W., and C. Wunsch (1998), Abyssal recipes II: Energetics of tidal and wind mixing, *Deep Sea Res., Part I*, *45*, 1977–2010.
- Nikurashin, M., and S. Legg (2011), A Mechanism for Local Dissipation of Internal Tides Generated at Rough Topography, *J. Phys. Oceanogr.*, *41*, 378–395.
- Pawlowicz, R., B. Beardsley, and S. Lentz (2002), Classical tidal harmonic analysis including error estimates in MATLAB using T\_TIDE, *Comput. Geosci.*, *28*, 929–937.
- Polzin, K. (2004), A heuristic description of internal wave dynamics, *J. Phys. Oceanogr.*, *34*, 214–230.
- Rainville, L., and R. Pinkel (2006), Baroclinic energy flux at the Hawaiian Ridge: Observations from the R/P FLIP, *J. Phys. Oceanogr.*, *36*, 1104–1122.
- Simmons, H. L. (2008), Spectral modification and geographic redistribution of the semi-diurnal internal tide, *Ocean Modeling*, *21*, 126–138.
- Staquet, C., and J. Sommeria (2002), Internal Gravity Waves: From Instabilities to Turbulence, *Annu. Rev. Fluid Mech.*, *34*, 559–593.
- Sun, O. M., and R. Pinkel (2013), Subharmonic Energy Transfer from the Semidiurnal Internal Tide to Near-diurnal Motions over Kaena Ridge, Hawaii, *J. Phys. Oceanogr.*, *43*, 766–789.
- Xie, X.-H., X.-D. Shang, H. van Haren, G.-Y. Chen, and Y.-Z. Zhang (2011), Observations of parametric subharmonic instability-induced near-inertial waves equatorward of the critical diurnal latitude, *Geophys. Res. Lett.*, *38*, L05603, doi:10.1029/2010GL046521.
- Yao, N. C. (1974), Bispectral and Cross-bispectral Analysis of Wind and Currents off the Oregon Coast, PhD dissertation, Oregon State University.
- Yao, N. C., S. Neshyba, and H. Crew (1975), Rotary Cross-Bispectra and Energy Transfer Functions Between Non-Gaussian Vector Processes I, Development and Example, *J. Phys. Oceanogr.*, *5*, 164–172.
- Zilberman, N. V., M. A. Merrifield, G. S. Carter, D. S. Luther, M. D. Levine, and T. J. Boyd (2011), Incoherent nature of M2 Internal Tides at the Hawaiian Ridge, *J. Phys. Oceanogr.*, *41*, 2021–2036.